The Impairment of Female Pelvic Ligaments and Its Relation With Pelvic Floor Dysfunction: Biomechanical Analysis

Sofia Brandão, Marco Parente, Ana Rita Silva, Thuane Da Roza, Teresa Mascarenhas, Isabel Ramos and R.M. Natal Jorge

Abstract Computational simulation of degeneration or damage on the structures that sustain the female pelvic organs may point to how they behave in real-life conditions. This work evaluated the effect of the impairment of female pelvic ligaments by means of numerical simulation considering rest and valsalva maneuver conditions. The model included the pelvic organs and several support structures, identified on magnetic resonance images from a young healthy female. For each tissue, material properties were obtained in the literature, and the best constitutive model was chosen for each structure. The displacement of the pelvic organs was assessed for normal ligaments, and also when their impairment was simulated by individually reducing their stiffness. The pelvic organs evidenced increased displacement when considering the damaged ligaments, similarly to what was found in previous imaging evidence. This model was suited for assessing ligaments damage. This is an important issue when simulating aging or trauma of the pelvic support structures.

Keywords Biomechanical simulation · Pelvic floor dysfunction · Ligament impairment

S. Brandão (✉) · T. Mascarenhas · I. Ramos
Centro Hospitalar de São João – EPE, Faculty of Medicine, University of Porto, Porto, Portugal
e-mail: sofia.brand@gmail.com

M. Parente · A.R. Silva · T. Da Roza · R.M. Natal Jorge
IDMEC-Pólo FEUP, Faculty of Engineering, University of Porto, Porto, Portugal
e-mail: rnatal@fe.up.pt

T. Da Roza
CIAFEL (Research Centre in Physical Activity, Health and Leisure), Faculty of Sport, University of Porto, Porto, Portugal

J.M.R.S. Tavares and R.M. Natal Jorge (eds.), *Computational and Experimental Biomedical Sciences: Methods and Applications*, Lecture Notes in Computational Vision and Biomechanics 21, DOI 10.1007/978-3-319-15799-3_4

1 Introduction

Female pelvic organs are grouped into anterior (bladder and urethra), central (vagina and uterus), and posterior (or anorectal) compartments. The spectrum of pelvic floor dysfunction depends on the compartment involved, and includes urinary incontinence (UI), constipation, and pelvic organ prolapse (POP), occurring in varying combinations. These are major issues among urologists and gynecologists. Farther, as they are also related with damage or weakness of the supports for the pelvic organs —provided by muscles, ligaments and fascia—its biomechanical analysis is also of interest to better understand the overall model of the disease.

The position and mobility of the structures of the anterior compartment are important to the study of UI. Loss of anterior vaginal support may result in urethral hypermobility, cystocele or anterior vaginal wall prolapse. The pubovesical, the pubourethral (PUL), and the uterosacral-cardinal muscles complex uphold the vesical and vaginal positions, as they stabilize the distal urethra, and maintain the cervix and the bladder base attached to the connective tissue of the fascia in the pelvic bones [1–4]. Damage or degradation of these apical supports is common in women with stress UI (SUI) and vaginal prolapse [5]. The normal position of the rectum is also maintained by the rectal fascia and the *levator ani* musculature [6]. Increased pressure in the proximal portion of the anal canal is supported by the puborectal muscle through vigorous contraction. To strengthen this effect, the iliococcygeal muscle firms the *levator plate* and the lateral ligaments of the rectum [7].

While physical examination, standardized questionnaires and imaging studies are the usual tools to assess pelvic floor dysfunction, computer simulation may also be used to learn and predict the biomechanical behavior of the pelvic structures under stress or after damage [8–10]. This is important in a clinical perspective, because the biomechanics involved in pelvic organ support is very difficult to evaluate experimentally. The finite element method (FEM) can be used to simulate pelvic floor muscles contraction against downward pressures that simulate intra-abdominal pressure or straining, as performed on dynamic magnetic resonance imaging (MRI) acquisitions. It allows testing pelvic floor muscles performance and compartmental stability when subjected to complex multidirectional forces. A study of Saleme et al. showed that a contraction intensity of 50 % would be necessary to avoid urine loss [11]. In addition, FEM can be used to mimic and predict vaginal delivery features and effects on pelvic floor muscles, illustrating true mechanical phenomena of one of the main causes of pelvic floor dysfunction. Interesting findings have been reproduced and reported, including that there is a mechanical response of the *levator ani* during the second stage of labor; muscle activation during vaginal delivery may represent an obstacle to fetal descent and increase the risk for pelvic floor injuries [12]; the shape of the head influences the mechanical response of the muscle; fetal head flexion during vaginal delivery may facilitate birth and protect the pelvic floor [13]; and increased fetal head diameter can influence medial *levator ani* portion to overstretch and injure, predicting injury patterns on predisposed women [14].

Few previous works focused the modeling of pelvic floor dysfunction in relation to damage in the support structures. Yip et al. [8] found that impaired pelvic floor muscles lead to vaginal and bladder neck prolapse. Additionally, Chen et al. reproduced anterior vaginal prolapse as related with progressive muscle and uterine ligaments damage [15, 16]. However, these studies focused on the middle compartment, but the whole pelvic cavity may suffer from ligament damage. Accordingly, this work evaluated the displacement of the pelvic organs considering the effect of the impairment on the pelvic ligaments. It was performed based on MRI of a healthy volunteer and numerical simulation using the FEM.

2 Method

The numerical model was built along several steps. The geometry of the pelvic organs and bones was obtained from MR images.

Some anatomical features of the PUL, uterosacral, cardinal and lateral rectal ligaments were confirmed in the literature [17]. The surfaces were meshed by rendering techniques using the software Inventor® (Autodesk, San Raphael, CA, USA) (Fig. 1).

A FE model (Fig. 2) was developed in Abaqus/CAE® software v. 6.12 (Dassault Systèmes Simulia Corp., Providence, RI, USA) (Fig. 2). The pelvic floor muscles were considered as a single mesh, while respecting its average 3-mm thickness. Material properties [18–20] and constitutive models were defined for each structure according to previous work, using the curve-fitting algorithms from the Abaqus®. The bones were fixed and considered as rigid, while the supportive structures were attached to the organs and bone using multi-point constrains (Abaqus® tie).

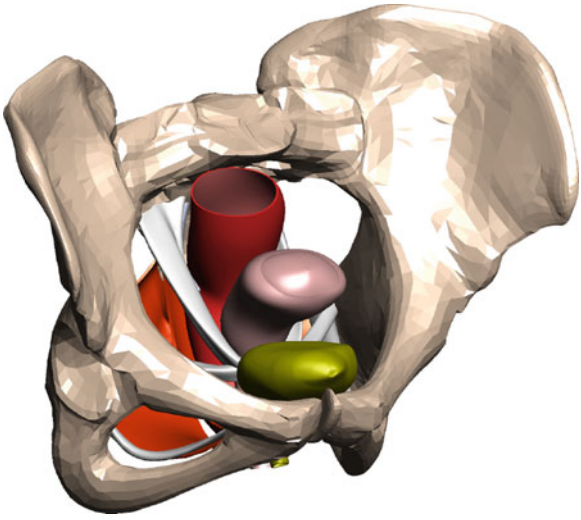

Fig. 1 3D model of the pelvis

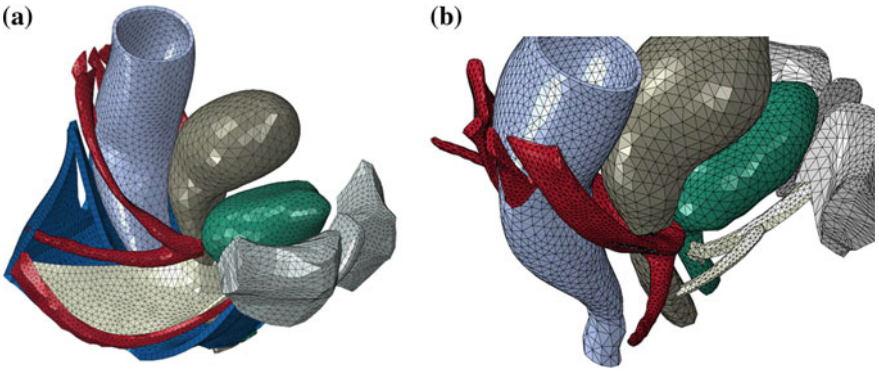

Fig. 2 Finite element model of the pelvis. The pelvic floor muscles and the pelvic fascia were excluded to better visualize the position of the pelvic ligaments

For the constitutive equation adopted in this work for the 3D passive and active behaviour of the pelvic floor muscles, a modified form of the incompressible transversely isotropic hyperelastic model used by Parente et al. [20], based on the work of Humphrey and Yin for passive cardiac tissues.

In the constitutive model, the strain energy per unit volume of the reference configuration can be written in the following form:

$$U = U_I\left(\bar{I}_1^C\right) + U_J(J) + U_f\left(\bar{\lambda}_f, \alpha\right) \tag{1}$$

where U_I,

$$U_I = c\left[e^{b\left(\bar{I}_1^C - 3\right)} - 1\right] \tag{2}$$

is the strain energy stored in the isotropic matrix, embedding the muscle fibres,

$$U_J = \frac{1}{D}(J-1)^2 \tag{3}$$

is the portion of the strain energy associated with the volume change and

$$U_f\left(\bar{\lambda}_f, \alpha\right) = U_{pas}\left(\bar{\lambda}_f\right) + U_{act}\left(\bar{\lambda}_f, \alpha\right) \tag{4}$$

is the strain energy stored in each muscle fibre, which can be divided into a passive elastic part and an active part due to the contraction. The passive elastic part U_{pas} is given by:

$$U_{pas} = A\left\{\exp\left[a\left(\bar{\lambda}_f - 3\right)^2\right] - 1\right\} \tag{5}$$

when $\bar{\lambda}_f > 1$, otherwise we consider the strain energy to be zero, assuming that the fibres offer no resistance to compression. The active part U_{act} is given by:

$$U_{act} = \alpha\, T_0^M \int_1^{\bar{\lambda}_f} 1{-}4\left(\bar{\lambda} - 1\right)^2 \mathrm{d}\bar{\lambda} \tag{6}$$

where α is the activation level, ranging from 0 to 1. When $0.5 < \bar{\lambda}_f < 1.5$, U_{act} is larger than 0, for other values of $\bar{\lambda}_f$ the muscle produces no force and, therefore, the strain energy is zero. The constant T_0^M is the maximum tension produced by the muscle at resting length $\left(\bar{\lambda}_f = 1\right)$.

In the above equation, T_0^M, c, b, A, a and D are constants [20], $\bar{I}_1^C$ is the first invariant of the right Cauchy-Green strain tensor with the volume change eliminated, i.e.

$$\bar{I}_1^C = \mathrm{tr}\,\bar{\mathbf{C}} = \mathrm{tr}\left(\bar{\mathbf{F}}^T\bar{\mathbf{F}}\right) = J^{-2/3}\mathrm{tr}\,\mathbf{C} \tag{7}$$

where $\bar{\mathbf{F}}$ is the deformation gradient with the volume change eliminated (Eq. 8)

$$\bar{\mathbf{F}} = J^{-1/3}\mathbf{F} \tag{8}$$

$\mathbf{F}$ is the deformation gradient and

$$J = \det\mathbf{F} \tag{9}$$

the volume change. Eq. (10) illustrates the fibre stretch ratio in the direction $\boldsymbol{N}$ of the undeformed fibre, given by:

$$\bar{\lambda}_f = \sqrt{\mathbf{N}^T\bar{\mathbf{C}}\mathbf{N}} = \sqrt{\bar{\mathbf{C}} : (\mathbf{N}\otimes\mathbf{N})} \tag{10}$$

where $\otimes$ denotes the tensor product.

The 2nd Piola-Kirchhoff stress tensor S can be obtained by the strain energy density given in Eq. (1), as:

$$\mathbf{S} = \frac{\partial U}{\partial \mathbf{E}} = \frac{\partial U_I}{\partial \mathbf{E}} + \frac{\partial U_f}{\partial \mathbf{E}} + \frac{\partial U_J}{\partial \mathbf{E}} \tag{11}$$

The Cauchy stress tensor σ is related to the 2nd Piola-Kirchhoff stress tensor $\mathbf{S}$ by

$$\sigma = J^{-1}\mathbf{F}\mathbf{S}\mathbf{F}^{T} \tag{12}$$

The material version of the tangent operator is defined as

$$\mathbf{H} = \frac{\partial^2 U}{\partial \mathbf{E}\,\partial \mathbf{E}} = \frac{\partial \mathbf{S}}{\partial \mathbf{E}} \tag{13}$$

and the spatial version can be obtained through a push-forward transformation

$$h_{ijkl} = \frac{1}{J} F_{im} F_{jn} F_{kp} F_{lp} H_{mnpq} \tag{14}$$

Muscles were assumed as having isotropic behavior, and the direction of the muscle fibers was assumed as being coincident with the direction of the maximum stress lines during deformation. Accordingly, a pressure of 1 kPa was applied in the inner surface of the pelvic cavity in order to obtain the direction of the fibers. Afterwards, the model was tested for supine rest (0.50 kPa) and supine valsava maneuver (4.00 kPa) conditions [10]. Mean values of magnitude displacement of the pelvic organs and pelvic floor muscles were evaluated when simulating healthy and progressive impaired support structures, by reducing material stiffness by 25, 50 and 75 %.

3 Results

The results from the magnitude displacement of the pelvic organs and pelvic floor muscles are presented on Table 1, and are illustrated on Figs. 3 and 4. The subtle pressure induced by the organs at rest lead to minor displacement of the pelvic floor muscles, upper portion of the bladder and uterus. When simulating valsalva maneuver, all the structures exhibited posterior and downward movement (Fig. 3b).

Table 1 Results from mean magnitude displacement from numerical simulation of rest, valsalva maneuver (VM) with healthy ligaments, and VM with different degrees of ligament impairment

Structure	Displacement (mm)	Rest	VM	VM, 25 % impairment	VM, 50 % impairment	VM, 75 % impairment
Uterus	min	0.48	1.86	3.61	4.54	6.16
	max	4.92	20.1	29.04	29.73	30.17
Bladder	min	0.61	2.6	4.8	5.5	6.59
	max	5.89	10.13	15.85	16.75	17.71
Rectum	min	0.11	0.34	0.53	0.66	0.98
	max	1.92	5.58	8.34	8.63	8.97
Pelvic floor	min	0	0	0	0	0
	max	4.25	11.65	17.14	17.42	17.41

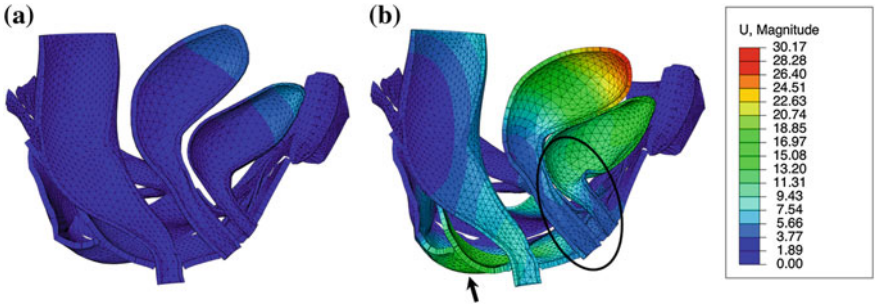

Fig. 3 Numerical simulation of valsalva maneuver. The basal pressure from the organ load was simulated on **a**, while the magnitude of the displacements for valsalva are illustrated on **b**

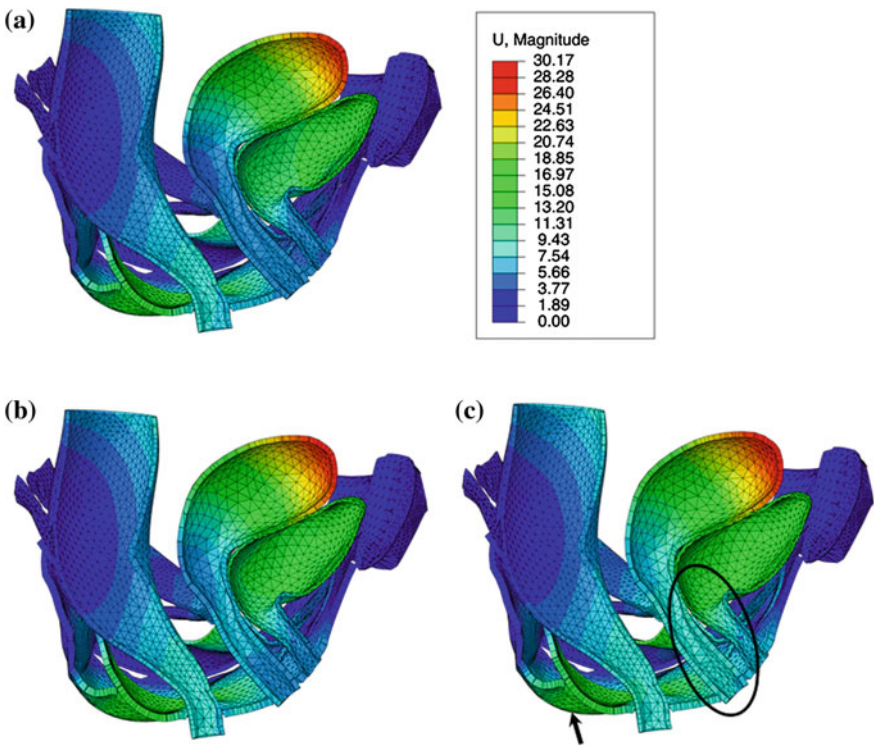

Fig. 4 Numerical simulation of Valsava Manuever, assuming 25 **a**, 50 **b**, and 75 % **c** reduction in ligament stiffness

The rectal portion of the pelvic floor muscles evidenced higher displacement than the anterior region, which was still not very evident when the support from the pelvic ligaments failed (Fig. 4c). Accordingly, the maximum displacement of the rectum was less than 4 mm from rest to valsalva maneuver, and 7.05 mm when

almost total damage of the pelvic ligaments was simulated. When considering the middle and anterior compartments, organs were more prone to descend, as indicated by the results on Table 1. The bladder and the uterus descended 11.82 and 25.25 mm, which is considerably more than the rectum. These results are in agreement with previous studies that evaluated the position of the pelvic organs for different stages of organ prolapse [21] and SUI [22] through MRI.

4 Discussion

UI requires integration of central and peripheral nervous systems, bladder wall and detrusor muscle, bladder neck, urethra, and pelvic support structures. Anteriorly, the PUL insert on the *arcus tendineus levator fascia* and in the inferior aspect of the pubic bone, assisting bladder neck opening during voiding [23]. The bladder neck position is influenced by connections between the puborectal muscle, vagina and proximal urethra. Additionally, the lateral ligaments of the bladder, and attachments to the cervix and anterior vagina provide postero-inferior support to the trigone.

SUI is characterized by involuntary urine leakage on effort or exertion, or during coughing [24] or exercise [24, 25]. Although its etiology is still an ongoing subject, it is mostly related to bladder neck hypermobility due to weakened or damaged pelvic floor muscles [26, 27], laxity of the fascia underlying the urethra, or damage of the pelvic ligaments [27–30]. Similarly, POP is common after injury to these support structures, which widens the *genital hiatus* and leads to organ prolapse, which may further stress or stretch ligaments. Hormonal changes are also related with weakened muscular and connective tissue support. A relation has been established between age and menopause, and degeneration of pelvic with estrogen receptors deficiency [31]. Moreover, progesterone is known to reduce muscular tonus of the ureters, bladder, and urethra because of its smooth muscle-relaxing and estrogen-antagonizing effects [32]. These features are typically seen in SUI and POP patients [27–30, 33, 34].

As the present results suggest, the bladder and uterus are the most affected by impaired ligaments. Despite the fact that the rectal portion of the pelvic floor seems to be the most movable (arrows on Figs. 3b and 4c), the puborectal muscle and the strong fascial involvement have a major role on maintaining rectal position. On the contrary, the urethra, the bladder neck, and the vagina get progressively compressed against the pelvic floor when the IAP is increased.

The FEM has been used by Marino et al. to study structural differences between lateral, trigone and anterior walls of the bladder, in correlation with the disposition of fibers of detrusor muscle and its thickness. When the simulation was performed in the absence of the PUL, the deflections of pelvic fascia modified the distributions of loads towards a centripetal orientation, which increases the stress over the perineal area and sphincter tract [35]. The author also confirmed the role of these ligaments between pubis and the cervix-urethra tract in dividing the global pressure load in the several components. Chen et al. confirmed the relevance of the *levator*

ani in cystocele formation, since the decreased muscle resistance to counteract the stretch when the IAP is increased widens the *genital hiatus*. As a consequence, the vaginal wall is exposed to higher pressure, which resulted in larger cystocele size. Their model also helped to illustrate the role of apical support. With muscle impairment present and the anterior vaginal wall subjected to a differential loading, the tensile load has to be resisted by both apical and paravaginal connective tissue supports, as an 80 % impairment in apical support resulted in a 33 % larger cystocele size [16].

A model developed by Yip et al. [8] was employed to evaluate the impact of pelvic muscular defect on the vaginal apex support and bladder neck support, features which relates to SUI. Simulation showed that the compromise of muscular contributed to the descend of those structures, whcih is commonly seen in patients patients with SUI.

Our results are similar to the ones from Yip et al. [8] and Chen et al. [15, 16], regarding the fact that the middle and anterior compartments are more dependent on the support role of the pelvic ligaments.

5 Conclusion

Numerical simulation of damage on the pelvic ligaments lead to increased downward movement of the pelvic floor muscles and pelvic organs. These features are similar to what happens after trauma or when the age and hormonal effects weaken organ support. The results from this study are similar to the imaging studies that regularly evaluate organ prolapse or UI.

Acknowledgments The authors gratefully acknowledge to the funding by CNPq—from Brazil government and the project Pest-OE/EME/LA0022/2013 and also to the project "Biomechanics: contributions to the healthcare", reference NORTE-07-0124-FEDER-000035 co-financed by Programa Operacional Regional do Norte (ON.2—O Novo Norte), through the Fundo Europeu de Desenvolvimento Regional (FEDER).

References

1. Tasali, N., et al., MRI in stress urinary incontinence: endovaginal MRI with an intracavitary coil and dynamic pelvic MRI. Urol J, 2012. 9(1): p. 397-404.
2. Kim, J. K., et al., The urethra and its supporting structures in women with stress urinary incontinence: MR imaging using an endovaginal coil. AJR Am J Roentgenol, 2003. 180(4): p.1037-44.
3. Pregazzi, R., et al., Perineal ultrasound evaluation of urethral angle and bladder neck mobility in women with stress urinary incontinence. BJOG, 2002. 109(7): p. 821-7.
4. Ramanah, R., et al., Anatomy and histology of apical support: a literature review concerning cardinal and uterosacral ligaments. Int Urogynecol J, 2012. 23(11): 1483-94.

5. Wang, L., L. Y. Hanand, and H. L. Li, Etiological study of pelvic organ prolapse and stress urinary incontinence with collagen status and metabolism. Zhonghua Yi Xue Za Zhi, 2013. 93 (7): p. 500-3.
6. Baert AL, Kanuth M (2008) Imaging Pelvic Floor Disorders. 2nd Revised Edition. Springer ISBN 978-3-540-71966-3.
7. Law, Y. M. and J. R. Fielding, MRI of pelvic floor dysfunction: review. AJR Am J Roentgenol, 2008. 191(S6): p. 45-53.
8. Yip, C., et al., A biomechanical model to assess the contribution of pelvic musculature weakness to the development of stress urinary incontinence. Comput Methods Biomech Biomed Engin, 2014. 17(2): p. 163-76.
9. Parente, M. P., et al., Deformation of the pelvic floor muscles during a vaginal delivery. Int Urogynecol J Pelvic Floor Dysfunct, 2008. 19(1): p. 65-71.
10. Noakes, K. F., et al., Subject specific finite elasticity simulations of the pelvic floor. J Biomech, 2008. 41(14): p. 3060-5.
11. Saleme, C. S., et al., An approach on determining the displacements of the pelvic floor during voluntary contraction using numerical simulation and MRI. Comput Methods Biomech Biomed Engin, 2011. 14(4): p. 365-70.
12. Parente, M. P., et al., The influence of pelvic muscle activation during vaginal delivery. Obstet Gynecol, 2010. 115(4): p. 804-8.
13. Parente, M. P., et al., Computational modeling approach to study the effects of fetal head flexion during vaginal delivery. Am J Obstet Gynecol, *2010.* 203(3): p. 217.e1-6.
14. Ashton-Miller, J. A., and J. O. L. DeLancey, On the biomechanics of vaginal birth and common sequelae. *Annu Rev Biomed Eng, 2009.* 11: p. 163-76.
15. Chen, L., et al., Interaction between Apical Supports and Levator Ani in Anterior Vaginal Support: Theoretical Analysis. Obstet Gynecol, 2006. 108(2): p. 324-32.
16. Chen, L., J. A., Ashton-Miller, and J. O. DeLancey, A 3-D Finite Element Model of Anterior Vaginal Wall Support to Evaluate Mechanisms Underlying Cystocele Formation. J Biomech, 2009. 42(10): p. 1371-7.
17. Patel U. Imaging and Urodynamics of the Lower Urinary Tract. Springer. 2010. © Springer-Verlag London Limited 2010. ISBN: 978-1-84882-835-3.
18. Rubod, C., et al., Biomechanical properties of human pelvic organs. Urology, 2012. 79(4): p. 968 e17–22.
19. Kirilova, M., et al., Experimental study of the mechanical properties of human abdominal fascia. Med Eng Phys, 2011. 33(1): p. 1-6.
20. Parente, M. P., et al., The influence of the material properties on the biomechanical behavior of the pelvic floor muscles during vaginal delivery. J Biomech, 2009. 42(9): p. 1301-6.
21. Lakenam, M. M., et al., Dynamic magnetic resonance imaging to quantify pelvic organ prolapse: reliability of assessment and correlation with clinical findings and pelvic floor symptoms. Int Urogynecol J, 2012. 23(11): p. 1547-54.
22. Tarhan, S., et al., The comparison of MRI findings with severity score of incontinence after pubovaginal sling surgery. Turk J Med Sci, 2010. 40 (4): p. 549-56.
23. Strohbehn, K., et al. Magnetic resonance imaging of the *levator ani* with anatomic correlation. *Obstet Gyneco, 1996.* 87(2): p. 277-85.
24. Abrams, P., et al., Reviewing the ICS 2002 terminology report: the ongoing debate. Neurourol Urodyn, *2009.* 28(4): p. 287-90.
25. Kruger, J. A., H. P. Dietz, and B. A. Murphy, Pelvic floor function in elite nulliparous athletes. Ultrasound Obstet Gynecol, 2007. 30(1): p. 81-5.
26. Simeone, C., et al., Occurrence rates and predictors of lower urinary tract symptoms and incontinence in female athletes. Urologia, 77(2): p. 139-46.
27. Dietz, H. P., and J. M., Simpson, *Levator* trauma is associated with pelvic organ prolapse. BJOG, 2008. 15(8): p. 979-84.
28. Wu, Q., et al., Characteristics of pelvic diaphragm hiatus in pregnant women with stress urinary incontinence detected by transperineal three-dimensional ultrasound. Zhonghua Fu Chan Ke Za Zhi, 2010. 45(5): p. 326-30.

29. Siracusano, S., R., Mandras, and E. Belgrano, Physiopathology of the pelvic elements of support in stress urinary incontinence in women. Arch Ital Urol Androl, 1994. 66(S4): p. 151-3.
30. Wei, J. T., and J. O. L. DeLancey, Functional anatomy of the pelvic floor and lower urinary tract. Clin Obstet Gyneco, 2004. 47(1): p. 3-17.
31. Scheiner, D., et al., Aging-related changes of the female pelvic floor. Ther Umsch, 2010. 67 (1): p. 23-6.
32. Copas, P., et al., Estrogen, progesterone, and androgen receptor expression in levator ani muscle and fascia. J Womens Health Gend Based Med, 2001. 10(8): p. 785-95.
33. Zhu, L., J. H. Lang, and R. E. Feng, Study on estrogen receptor around levator ani muscle for female stress urinary incontinence. Zhonghua Fu Chan Ke Za Zhi, 2004. 39(10): p. 655-7.
34. Tinelli, A., et al., Age-related pelvic floor modifications and prolapse risk factors in postmenopausal women. Menopause, 2010. 17(1): p. 204-12.
35. Tinelli, A., et al., Age-related pelvic floor modifications and prolapse risk factors in postmenopausal women. Menopause, 2010. 17(1): p. 204-12.